Effects of Physical Heterogeneity on the Adsorption of Poly(ethylene oxide) at a Solid−Liquid Interface

Yu-Wen Huang and Vinay K. Gupta*

Department of Chemical Engineering, University of Illinois, Urbana−Champaign, 600 S. Mathews Avenue, Urbana, Illinois 61801

Received October 16, 2000; Revised Manuscript Received February 7, 2001

ABSTRACT: Experiments on the adsorption of PEO from aqueous solutions onto planar surfaces that are physically heterogeneous but chemically homogeneous are presented. Gold substrates that differ only in the degree of roughness were prepared by thermal evaporation on glass and by template stripping from mica. To ensure a similar chemical interface, the gold substrates were modified with a self-assembled monolayer of a long chain alkanethiol ($CH_3(CH_2)_{11}SH$). The kinetics of adsorption of PEO were monitored using a surface plasmon resonance technique with high time resolution. The experimental measurements demonstrated that higher adsorbed amounts and lower chain distortion accompanied an increase in surface roughness. These are the first systematic experimental measurements that substantiate past theoretical predictions of polymer adsorption on random surfaces. Kinetic studies revealed that the initial rate of adsorption was proportional to bulk concentration on both rough and smooth substrates, but the PEO adsorbed more readily on the rougher surfaces.

Introduction

Preparation of adsorbed polymer layers is an important step in many applications.[1−3] For example, adsorption of polymers plays a significant role in controlling surface adhesion, achieving biocompatibility of surfaces, stabilization of colloidal dispersions such as paints and inks, and thin-layer chromatography.[1,4] This widespread applicability of polymer adsorption has spurred numerous theoretical and experimental investigations on the subject of polymer adsorption onto a solid surface.[3] While great strides have been made in characterization and understanding of the structure and dynamics of adsorbed polymer layers, much less attention has been focused on the influence of surface heterogeneity on polymer adsorption.

In real surfaces, nonuniformities exist in the form of topological roughness of the solid interface, *"physical heterogeneity"*, and in the form of distribution of surface sites that show different energetic interactions with a polymer, *"chemical heterogeneity"*. It is generally accepted that both types of surface heterogeneity play a critical role in determining adsorption characteristics of a polymer. Motivated by the importance of surface heterogeneity, several recent theoretical studies have focused on the influence of each type of heterogeneity on the adsorption behavior of polymeric chains.[5−12] However, corroboration by systematic and well-defined experiments is virtually nonexistent.[13]

In the past, one of the major stumbling blocks for experiments on the effect of surface heterogeneity on polymer adsorption has been the inability to prepare well-defined surfaces, meticulously and reproducibly, that are either chemically homogeneous but physically heterogeneous or vice versa. Now, however, there exists an unprecedented capability to design and tailor surfaces at the molecular level by using self-assembly of molecules.[14,15] We have used this novel capability and focused on experimental characterization of the influence of heterogeneity on the adsorption behavior of polymers. In this paper, we present the results of our experiments on adsorption of poly(ethylene oxide) (PEO) on solid surfaces that are chemically similar but differ in their physical roughness.

Because roughness is ubiquitous in practical applications of polymer adsorption, several early theoretical studies analyzed the effects of physical heterogeneity on polymer adsorption. In these studies the rough surfaces were modeled as random,[16] fractal,[8,11] sinsuodial gratings,[5,6] or corrugated surfaces.[17] Pioneering works by Baumgartner and Muthukumar,[9] Edwards and Muthukumar,[18] Douglas,[8] and others came to a common consensus that increasing interfacial roughness enhances adsorption. In these studies, simple physical arguments stated that increasing the surface roughness increases the probability of polymer−surface intersection and thereby enhances the number of polymer−surface interactions relative to an ideal planar interface. Furthermore, the loss of configurational entropy of the polymer chain was hypothesized to be less on a rough surface. Thus, these theoretical studies predicted that adsorption occurs more readily on rough surfaces and that the adsorbed amount of the polymer increases due to the effects of physical heterogeneity. These arguments have been supported by a number of more recent analyses of adsorption of polymers on random or structured surfaces using methods such as scaling analysis, Monte Carlo simulations, and replica-field theory.[7,10,19] We know of no experiments that have studied the effect of roughness on polymer adsorption at planar surfaces.

Classical methods for measuring polymer adsorption rely on suspensions of colloidal particles in polymer solutions and characterization of the polymer concentration in the supernatant. Because this method permits neither in-situ studies of structure/thickness of the adsorbed layer nor control over the nature of the solid surface, macroscopically planar surfaces are more suited to polymer adsorption studies. Planar surfaces are easier to model theoretically, but their low specific areas necessitate sensitive methods of measurement for moni-

* To whom correspondence should be addressed. E-mail vgupta@uiuc.edu; Fax 217-333-5052; Tel 217-244-2247.

10.1021/ma001780z CCC: $20.00
Published on Web 04/19/2001

toring polymer layers that are a few tens of angstroms in thickness. Past studies have used a variety of techniques based on the interference, reflection, or absorption of light, the scattering of neutron or X-ray beams, or nuclear magnetic resonance (NMR).[20,21] Methods based on X-ray scattering or neutron reflection probe the adsorbed layers at nanometer length scales and yield structural information such as density profiles for the adsorbed layers. However, these methods are not easily applicable to kinetic measurements due to factors such as high absorption in the condensed solvent phase, low fluxes, and long time averaging to obtain high signal-to-noise ratio. Similarly, FTIR-based methods while being chemically specific can have limitations due to necessity of IR transparent solvents and IR transparent substrates (for attenuated total reflection).[21] In contrast, optical methods such as ellipsometry[22] and reflectometry[23−25] are easier to implement and facilitate rapid, noninvasive characterization of adsorption at surfaces. However, these optical methods are sensitive primarily to the thickness of adsorbed polymer.

Our experiments on the adsorption of PEO are performed on gold-coated substrates that support a self-assembled monolayer (SAM) formed from methyl-terminated alkanethiol. These surfaces offer several advantages for performing well-defined experiments on polymer adsorption. First, it is possible to prepare gold substrates that have different degrees of roughness. Second, the SAM formed on the two types of gold substrates provides an identical chemical interface of densely packed methyl (CH_3) groups that can be created easily and reproducibly. In past work on silica surfaces, difficult procedures such as silanization have been used which do not always give the same chemical interface unless careful control is exercised.[26] Silver or aluminum surfaces are prone to oxidation and are therefore not ideal. Third, gold substrates permit the use of noninvasive and in-situ surface sensitive techniques such as surface plasmon resonance (SPR) to monitor the kinetics of adsorption.[27]

In this paper, we discuss results of PEO adsorption on ultraflat template-stripped gold[28] substrates that are smooth (roughness ∼3 Å) and on gold evaporated onto glass substrates that have roughness ∼8 Å. We demonstrate that both substrates are chemically similar after modification by SAMs formed from dodecanethiol ($CH_3(CH_2)_{11}SH$) but possess a subtle physical heterogeneity due to the underlying gold substrate. Scanning tunneling microscopy (STM) of the gold substrates is presented for analysis of the topography of the surfaces.[29] A description of the SPR apparatus that we use to perform in-situ surface specific analysis with high time resolution is provided. Adsorption isotherms for PEO as well as the kinetics data on both ultraflat and rough gold substrates are presented and discussed in the context of available theoretical models.

Experimental Section

Chemicals. The ethanol used in monolayer preparation was absolute 200 proof (Aaper Alcohol and Chemical Co., KY). Hexadecane used for contact angle measurements was reagent grade (Fisher Scientific, PA). 11-Dodecanethiol used for formation of self-assembled monolayers was purchased from Aldrich (Milwaukee, WI). Both hexadecane and dodecanethiol were passed through a column of neutral alumina before use. Monodisperse poly(ethylene oxide) was purchased from Polymer Source, Canada. According to the supplier, the PEO chains contained hydroxyl groups on both ends, and the molecular weight (M_w) was 53.5K with $M_w/M_n = 1.07$. Purified water was from an EasyPure UV system (Barnstead, IA). PEO was dissolved in pure water and stirred overnight to make stock solutions of 100 ppm (by weight) concentration. Solutions of lower concentrations were prepared by a series of dilutions.

Preparation of Surfaces. Gold substrates on glass (hereafter referred to as "rough substrates") were prepared on microscope glass slides (Fisher's Finest Premium) by thermal evaporation. A 20 Å adhesion layer of chromium (Kurt Lesker, PA) was first deposited at 0.3 Å/s. Subsequently, 500 Å gold (99.999% purity) was deposited at 5 Å/s under a pressure of 4×10^{-6} Torr.

Smooth gold substrates (hereafter referred to as "ultraflat substrates") were prepared by template stripping evaporated gold from mica as per the procedure reported in the literature.[28] 1 in. × 3 in. sheets of PELCO mica were purchased from Ted Pella, CA. Freshly cleaved mica sheets were placed in the thermal evaporator and annealed under vacuum ($<10^{-6}$ Torr) at 100 °C for 6 h. 600 Å of gold was evaporated onto the annealed mica substrates at a rate of 1 Å/s. After cooling the substrates, a thin layer of an optically clear epoxy, Epotek 301-2 (Epoxy Technology, MA), was spread on the gold and sandwiched between the gold-coated mica and a glass slide. The sandwiched substrate was cured in a vacuum oven for 3 h at 80 °C. The gold layer in contact with the mica surface was carefully stripped by using mechanical force before use.

For preparation of monolayers, substrates were rinsed with ethanol and then immersed in 1 mM ethanolic solutions of dodecanethiol for a period of several hours to overnight. The SAMs were rinsed extensively with ethanol and blown dry with nitrogen.

Characterization of Substrates and SAMs. The bare gold substrates were characterized by scanning tunneling microscopy using a Nanoscope IIIa multimode AFM (Digital Instruments, CA) equipped with a low-current amplifier with 10^{11} gain and 4 kHz filter. Mechanically cut Pt−Ir tips supplied by Digital Instruments were used. STM images were acquired using an E-scanner. To compare the average roughness and fractal dimension of the substrates, images were acquired at multiple locations of different samples using the same tip. Software supplied by Digital Instruments (Nanoscope, version 4.23b15) was used to analyze the images.

The chemical interface of the SAMs was characterized using contact angle measurements. Contact angles were measured using a Ramé-Hart goniometer (model 100-00). Three pairs of advancing and receding angles were measured for each drop. At least two separate drops were used for each surface; the reported angles are an average of all (six or more) measurements for that sample. Hexadecane was used as the probe liquid.

Surface Plasmon Resonance Apparatus. Briefly, the surface plasmon resonance technique is based on the resonant excitation of the surface polaritons in a thin (∼500−600 Å) metallic gold layer by an evanescent optical field.[30] The evanescent optical field is generated by the total reflection of light at the internal surface of a prism, which is in optical contact with the thin gold film. At a certain angle of incidence, called the surface plasmon resonance angle (θ_p), a minimum in the total reflectivity of p-polarized light is observed. The angle, θ_p, depends on the dielectric environment of the exposed gold surface, and adsorption on the gold surface shifts θ_p to higher values.

We used a home-built surface plasmon instrument (Figure 1) in the Kretschmann configuration[31] that was based on a design reported in the literature.[32] A 3 mW helium−neon laser diode (Thor Labs, NJ) of wavelength 670 nm was used as the light source. The light was polarized along the p-polarization direction using a dichroic polarizer. A half-wave retarder plate (HWP) was placed in the beam path to rotate the polarization by 90° and switch between s-polarized and p-polarized light without variation in the intensity of incident light. An electronic optical scanner (Electro-optical Products, model SC-20) was utilized to allow an angular scan of the laser beam through various angles of incidence. A planocylindrical lens directed the light on the curved surface of a half-cylinder made of SF10

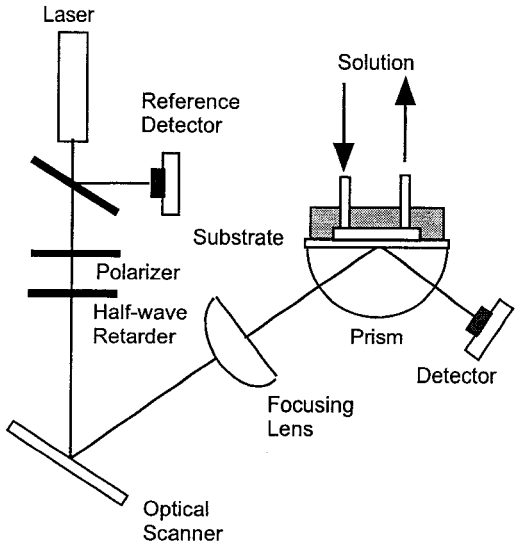

Figure 1. Schematic illustration of the surface plasmon resonance apparatus.

glass. The angle-dependent light intensity of the reflected light was monitored using a silicon photodetector (PDA55, Thor Labs, NJ).

Index matching fluid (No.16242, Cargille, NJ) was used to obtain optical contact between the gold-coated substrate and the prism. A flow cell measuring 7 mm × 15 mm × 0.7 mm was machined in Teflon and mounted onto the gold substrate and prism using a Kalrez O-ring. Before an adsorption run, the cell and tubes were cleaned with piranha solution at 70 °C for 40 min and then rinsed with copious amounts of pure water. **Warning:** piranha solution should be handled with caution; it can detonate unexpectedly.[33]

Fluids were pumped through the flow cell with a peristaltic pump (P-07523-40 and P-77390-00, Cole-Parmer, IL) with Teflon tubing. First, ethanol was pumped through to clean the surface, and the ethanol was removed by pumping a large quantity of pure water. Once a stable baseline was reached, the flow was switched to the PEO solution. The flow rate was fixed such that a shear rate of approximately 6 s^{-1} was achieved to limit the role of diffusion-controlled mass transport. The temperature of water and PEO solutions was maintained at 20 °C throughout the experiment by a recirculating water bath. When a plateau in the adsorption of PEO was reached, the surface was rinsed with pure water.

Data Acquisition and Processing. Synchronized data acquisition of the detector signal was done on a Pentium PC using a program written in HPVee 4.0 (Agilent Technologies, CO). During a half-cycle ($0 < t < T/2$; $T = 16.64$ ms) of the mirror scan, the SPR angle θ_p was traversed twice, and two minima observed at t_1 and t_2 in the measured intensity of the reflected light. Typically, the driving voltage was set such that the mirror scanned an angular range of 0.83°. In addition to recording the reflectivity curve over the complete angular range, we used an analog differentiator circuit and a digital timer (resolution = 5 μs) to track the time difference ($\tau = t_2 - t_1$) between the two minima in the reflected intensity. This change in τ is proportional to the shift in the SPR angle and is thereby a direct measure of the adsorption at the gold−solution interface. Because we used an electronic optical scanner, the angular scan took approximately 16 ms, and processing and recording of each data point could be completed within approximately 400 ms. This is significantly faster than measurement times reported in past studies using reflectometry or ellipsometry and allows us to monitor the rapid rates of adsorption at high bulk concentrations of the polymer.

The reflectivity in the surface plasmon experiment was fit to an optical model based on Fresnel equations. We used a five-layer model[34] for the epoxy (or glass), gold, SAM, polymer, and water system. The normalized reflectivity was obtained by ratio of the reflectivity of the p-polarized light with the s-polarized light. Because s-polarized light does not couple to the surface plasmon wave, such normalization corrected the deviations from the optical components for the scanning of the laser. Nonlinear least-squares fitting was performed by a Levenberg−Marquardt algorithm using IgorPro software (WaveMetrics, OR).

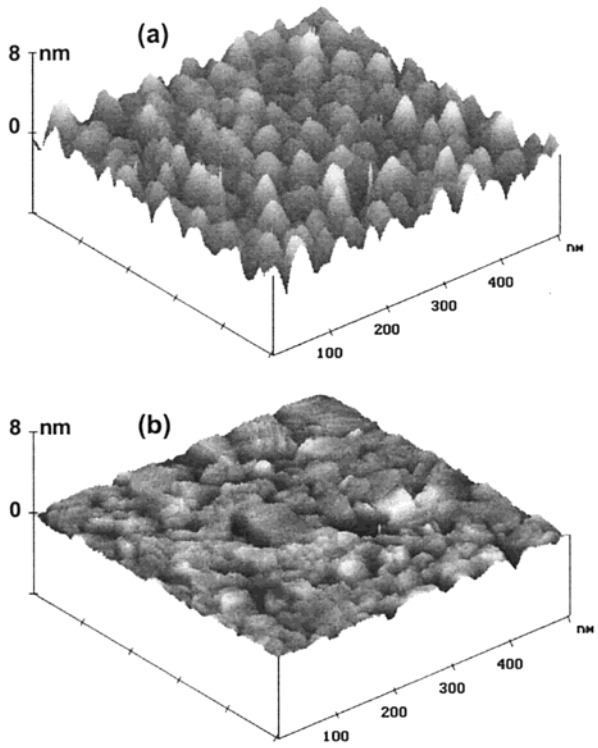

Figure 2. Scanning tunneling microscopy of (a) rough gold substrates prepared by thermal evaporation of gold on glass and (b) ultraflat gold substrates prepared by template stripping technique.

Results and Discussion

Characterization of the Substrates. By using scanning tunneling microscopy, the surface topography of the gold substrates can be characterized. Figure 2 shows surface plots of the ultraflat gold substrate and the rough gold substrate. In contrast to the ultraflat gold substrate (Figure 2b), the rough gold substrate shows a pebbly texture where the gold grains are about 20−30 nm in diameter (Figure 2a). The images readily reveal that the ultraflat substrates possess smaller deviations in height.

The qualitative features revealed in the STM images can be quantified using a surface roughness value. Even though no universally accepted mathematical definition of surface roughness exists, statistical parameters can be used to define roughness and are useful for relative measurements.[35] One measure of the roughness is the root-mean-square (R_{rms}) deviation of the heights of the various features imaged by STM. Our estimated R_{rms} is based on the expression

$$R_{rms} = [(Z_1^2 + Z_2^2 + Z_3^2 + ... + Z_N^2)/N]^{0.5}$$

where Z_i are the height deviations from the data plane. Table 1 shows the estimated values of the R_{rms} for both gold substrates. The template stripped, ultraflat gold substrates show values of less than 3 Å, which indicates that the surface corrugation on these substrates is low.

Table 1

	rough gold substrates	ultraflat gold substrates
R_{rms}	8.2 ± 0.26 Å	2.7 ± 0.28 Å
D	2.25 ± 0.02	2.15 ± 0.03
θ_a	46 ± 1°	47 ± 1°
θ_r	42 ± 1°	46 ± 1°
L_{ads}	12.1 ± 0.2 nm	14.7 ± 1.0 nm

The thermally evaporated rough gold substrates are slightly more corrugated and show $R_{rms} \sim 8$ Å.

Another way to analyze the geometric complexity of the surfaces is via a fractal analysis.[36] For a fractal surface, the fractal dimension (D) lies between 2 and 3. For a perfectly flat surface $D = 2$, and for rougher surfaces the value is higher. Table 1 shows that the fractal dimension of both gold substrates is only slightly higher than 2, indicating that these surfaces are largely flat.[37] There is a slight difference in D for the two substrates, and the rough gold surface shows a higher fractal dimension. Thus, both R_{rms} and D indicate that small differences in roughness exist at the nanometer length scale, which is commensurate with the typical size of a polymer chain.

Self-assembled monolayers of $CH_3(CH_2)_{11}SH$ were formed on both gold substrates. The methylated surfaces are low-energy surfaces and are therefore less prone to contamination. The advancing contact angles of hexadecane on both surfaces were measured to be 46°−47° and are consistent with values reported for a hydrophobic interface of densely packed CH_3 groups.[15,38] The matching advancing angle is evidence that both surfaces possess the same chemical interface and homogeneity. There is a measurable decrease of 4° in the receding contact angles for the monolayers supported on the rough gold substrate, which is consistent with the higher roughness of these substrates.[39]

PEO Adsorption. Typical reflectivity profiles measured using the SPR apparatus before and after adsorption of PEO are shown in parts a and b of Figure 3 for the ultraflat gold substrate and rough gold substrate, respectively. Because the granular structure of an evaporated gold layer can give rise to loss mechanisms such as scattering, the widening of the reflectivity curve around the minimum in Figure 3b is consistent with the higher roughness of these substrates.[30] Past studies have shown that, for ultrathin dielectric layers of thickness less than 100 Å, independent determination of both refractive index and thickness from the surface plasmon experiments is not possible unless multiple solvents or multiple wavelengths are used.[40] Therefore, in fitting the adsorbed polymer layer, we assumed a constant refractive index of $n_p = 1.36$, which is consistent with past reports of low (~20-30%) mass fraction of PEO in adsorbed layers.[41] The small difference between n_p and the refractive index of water (~1.3309) reflects large hydration of the PEO layer.

PEO has been reported to adsorb with high affinity on hydrophobic and hydrophilic silica surfaces.[23,25] Results in Figure 4 show that the maximum surface excess of PEO (Γ_{max}) was similar at low and high bulk concentrations on the rough gold substrates, which is consistent with high affinity type behavior. Figure 4 also shows that the adsorbed PEO is retained on the surfaces even after rinsing the adsorbed layers with pure water. The slight decrease in the adsorbed material, primarily, for the highest concentrations indicates that here some polymer chains can be loosely bound. For bulk solution concentrations ranging from 0.1 to 50 ppm the maximum surface excess was between 0.75 and 0.82 mg/m^2 (Figure 4). In comparison, Pagac et al.[42] have reported saturation amounts of 0.52 mg/m^2 for PEO of a much

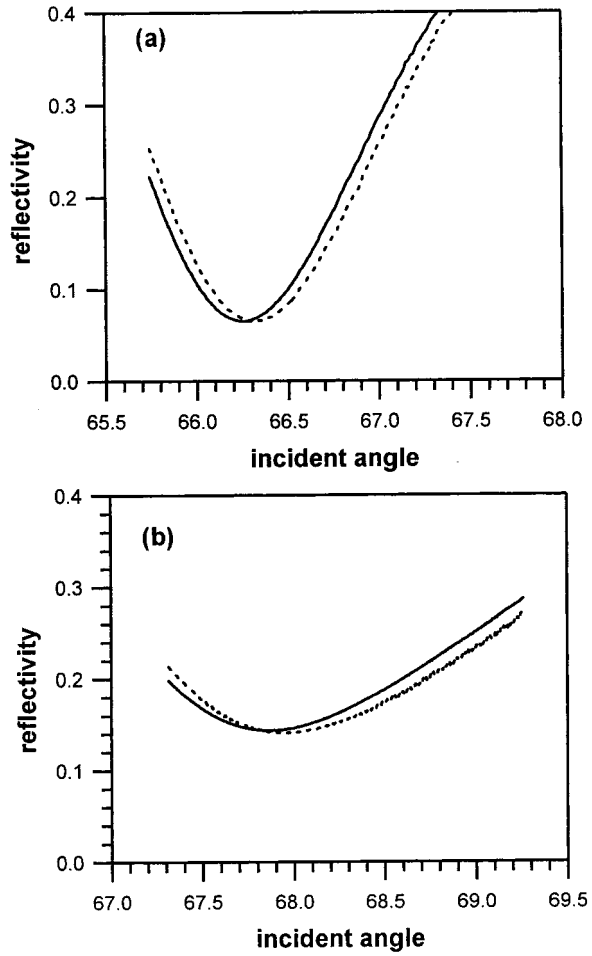

Figure 3. Reflectivity of p-polarized light obtained before (solid line) and after (dashed line) adsorption of PEO on (a) ultraflat gold substrates and (b) rough gold substrates.

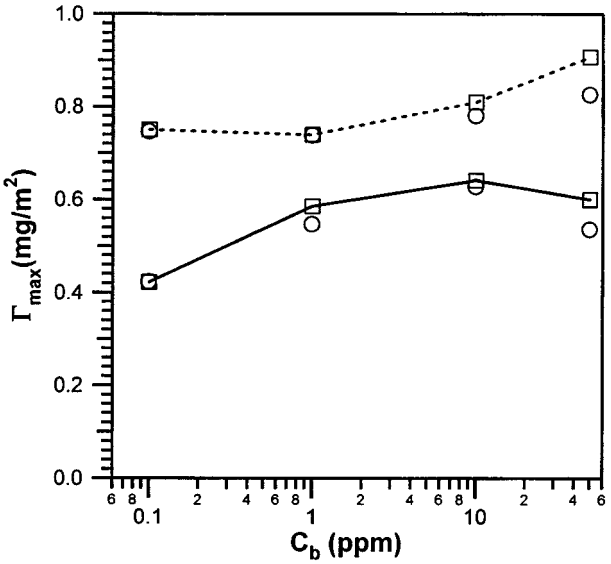

Figure 4. Maximum adsorbed amount of PEO as a function of the bulk solution concentration for ultraflat gold substrates (solid line) and rough gold substrates (broken line). Square symbols represent the adsorbed amount in contact with PEO solution while circles represent the amount of PEO retained after rinsing with pure water. The solid and dashed lines are drawn to simply guide the eye.

higher molecular weight ($M_w = 420$K) on silicon wafers silanized with trimethylchlorosilane (TMS). On hydrophilic surfaces Dijt and co-workers[23] have reported Γ_{max} values of 0.52 mg/m^2 for PEO ($M_w \sim 56.3$K) while Fu and Santore[25] reported a value of 0.35 mg/m^2 for PEO ($M_w \sim 32.6$K). In preliminary work on hydrophilic SAMs of $HOOC(CH_2)_2SH$ supported on the ultraflat gold substrates, we have found that Γ_{max} was much smaller ($\sim$0.1 mg/m^2) and indicative of a highly flattened conformation of the PEO chain on the surface.[43]

Comparison of our results with past reports is difficult because few studies have reported characterization of surface properties such as topological roughness or chemical functionality.[44] For example, the origin for the higher Γ_{max} on the methylated gold substrates compared to results by Pagac et al. is complicated because it is possible that the surfaces used by Pagac et al. did not possess a dense array of methyl (CH_3) groups at the interface. Pagac and co-workers report $\theta_{a,water}$ to be 54° on the surfaces that they used in their investigation, which is not consistent with literature reports of contact angles on TMS monolayers. Recently, Fadeev and McCarthy[45] have prepared TMS monolayers by carefully controlling solvent, temperature, and surface hydrolysis and have demonstrated that a dense interface of methyl (CH_3) groups in these monolayers will show $\theta_{a,water}$ to be 105°−108°. Comparison of results on the hydrophobic SAMs formed from $CH_3(CH_2)_{11}SH$ with the hydrophilic SAMs formed from $HOOC(CH_2)_2SH$ shows that Γ_{max} is smaller on the latter surfaces. The results of Fu and Santore,[25] who used hydrophilic silica surfaces that were carefully characterized, also support this trend.

Figure 4 shows the variation in Γ_{max} on two surfaces that possess the same degree of hydrophobicity (as indicated by the $\theta_{a,hexadecane}$ in Table 1) but different surface roughness. Γ_{max} shows a slightly larger deviation between low and high bulk concentrations on the ultraflat gold substrates. Specifically, Γ_{max} dropped from 0.5 to 0.6 mg/m^2 at high bulk solution concentrations (10−50 ppm) to approximately 0.4 mg/m^2 at 0.1 ppm. More interestingly, the maximum surface excess of PEO was 20−30% lower on the ultraflat gold substrates compared to the rough gold substrates. Because the two substrates differ only in the physical roughness and not in the chemical nature of the surface, these results indicate that the maximum surface excess of the polymer increases due to the presence of physical heterogeneity. The results in Figure 4 represent the first experimental corroboration of the predictions of the theoretical studies on interactions of a polymer on rough and smooth planar surfaces.[6,8−10,18,19]

From the data shown in Figure 4, we can estimate the surface area occupied by each PEO chain on the solid surface as

$$A_{ads} = M_w/(\Gamma_{max} N_A)$$

where M_w is the molecular weight and N_A is Avogadro's number. The characteristic size of the polymer chain parallel to the surface is then

$$L_{ads} = (4A_{ads}/\pi)^{0.5}$$

Using these expression, the estimated L_{ads} is listed in Table 1 for the ultraflat and rough gold substrates. The radius of gyration of the PEO ($M_w = 53.5$K) chain in free solution is approximately 11.6−12.3 nm.[46] Comparison with the estimated value of L_{ads} (Table 1) shows that the polymer chain is slightly flattened on the ultraflat gold substrate relative to its size on the rough gold substrates. Thus, there is smaller distortion of the polymer chain upon adsorption on rougher surfaces. Past theoretical models of adsorption of polymer chains on random surfaces and structured surfaces have proposed such an effect.[8,9] It is also evident that PEO, which is a hydrophilic polymer, does not flatten significantly on both hydrophobic surfaces.

Kinetics of Polymer Adsorption. To follow the adsorbed mass of PEO as a function of time, we exploited the high time resolution of our surface plasmon apparatus. Figure 5 shows $\Gamma(t)$ for adsorption from solutions of several bulk concentrations of PEO. The general characteristics of $\Gamma(t)$ in Figure 5 are similar to adsorption kinetics reported for most homopolymers.[3] Adsorption proceeds rapidly at the bare surface, and Γ increases linearly with time. When competition for space at the surface becomes dominant, the rate of adsorption decreases, and eventually $\Gamma(t)$ reaches a plateau at long times. Figure 5 also reveals that the initial rate of adsorption, $(d\Gamma/dt)_0$, increases as the bulk concentration is increased, and for $C_b > 1$ ppm the rate of adsorption is such that within 100 s the surface coverage reaches 70% of Γ_{max}. For adsorption from solutions with high C_b, there is a sudden onset of a plateau after the initial rapid rise in $\Gamma(t)$, and the adsorption seems to be close to equilibrium. However, this sudden slowing in the rate of adsorption is followed by gradual increase in $\Gamma(t)$, and the system appears to be close to saturation only at very long times. Similar kinetic curves have been reported in the literature, but no clear physical picture is available at this time to explain the behavior. Conformational reorganization processes of the polymer chain can, plausibly, give rise to time-dependent changes in Γ.

The effect of physical heterogeneity is clearly observed in these kinetic data. For the lower concentrations (Figure 5a,b), the initial rate of adsorption is smaller on the ultraflat gold substrates, indicating that PEO adsorption occurs more readily on the rough gold substrates. However, it becomes progressively difficult to observe the difference in the initial rate of adsorption at high concentrations. Figure 5c,d shows that at short times the rise in $\Gamma(t)$ for the rough gold substrates is superimposed on the rise in $\Gamma(t)$ for the ultraflat gold substrates, but the adsorbed amount at the plateau differs.

Currently, no detailed theory exists for kinetics of adsorption, and therefore, we interpret the differences in $(d\Gamma/dt)_0$ in the context of a model that has been frequently employed in past studies.[3,47] In this model, the adsorption kinetics are subdivided into transport to the surface, attachment, and spreading on the surface. The convective flux (J), which can be written as

$$J = k(C_b - C_{surf})$$

where k is the rate constant of adsorption and depends on the hydrodynamic conditions while C_{surf} is the subsurface concentration, and it depends on the attachment of the polymer chains to the surface as well as their conformational rearrangements. No laws exist for determining the value of C_{surf}. Under a pseudo-steady-state assumption, it is typically assumed that C_{surf} changes negligibly at early time and $(d\Gamma/dt) = J$. In the case of high affinity adsorption behavior, C_{surf} is small during the initial period of adsorption, and $(d\Gamma/dt)_0$ is expected to be constant and linearly proportional to C_b.

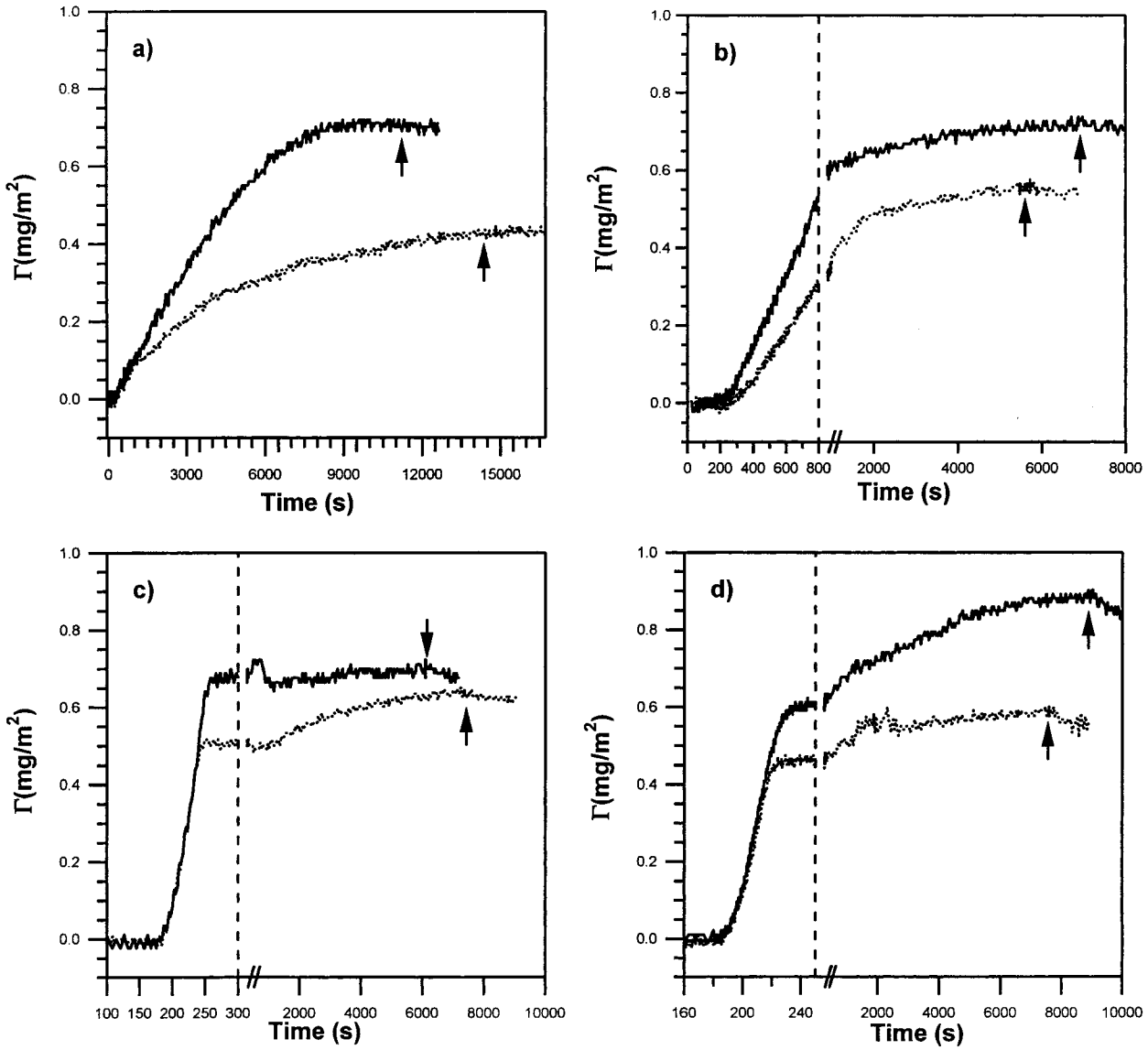

Figure 5. Kinetics of PEO adsorption from aqueous solutions at varied bulk solution concentrations: (a) $C_b = 0.1$ ppm; (b) $C_b = 1$ ppm; (c) $C_b = 10$ ppm; (d) $C_b = 50$ ppm. The solid curve represents adsorption on rough gold substrates and the dashed curve on ultraflat gold substrates. The arrow indicates the point at which the adsorbed layers were rinsed with pure water. For plots in (b)−(d), short time and long time behavior is shown on two different scales.

The effects of attachment and spreading in the kinetics of adsorption have also been considered using physical arguments and simple models.[47] To discern the effects of attachment, one commonly held scenario assumes that the attachment rate of the polymer chains is much higher than the detachment rate, and C_{surf} can be related to $d\Gamma/dt$ through a first-order process (KC_{surf}). The rate of adsorption is then

$$d\Gamma/dt = kC_b/(1 + k/K)$$

where K is some kinetic coefficient characteristic of the attachment barrier on the surface. The effect of an attachment barrier is then to lower the flux from the limiting value of kC_b. To explore the effect of spreading of polymer chains, simple models[47] use the notion that flattening of the polymer chain on the surface to increase the number of segment−surface contacts leads to higher area per chain and lower adsorbed amount. The rate of this spreading and its manifestation in the kinetics are found to depend intricately on the mass transport rates.

The estimated initial slope $(d\Gamma/dt)_0$ for the runs with different bulk concentrations in our experiments is shown in Figure 6. Because the rate of adsorption on the ultraflat gold substrates for $C_b = 0.1$ ppm was very slow, only a small initial region of the $\Gamma(t)$ curve was used. Figure 6 shows that the initial rate, $(d\Gamma/dt)_0$, is approximately linearly proportional to the bulk concentration at all but the highest concentration that we studied.[48] This linear dependence is consistent with the pseudo-steady-state, convective model described above. We interpret the lower values for $(d\Gamma/dt)_0$ for ultraflat substrates compared to the rough gold subtrates as follows. The existence of a higher attachment barrier on the ultraflat gold substrates, i.e., a lower relative value of K, could account for the lower $(d\Gamma/dt)_0$. However, K should be independent of the bulk concentration, and the difference in $(d\Gamma/dt)_0$ should persist even when C_b is high. Because we do not observe lower $(d\Gamma/dt)_0$ at $C_b > 1$ ppm, we believe that attachment barriers, if any exist, are similar on both types of gold surfaces. The trends we see in $(d\Gamma/dt)_0$ are more consistent with a physical picture based on the effects of spreading. The

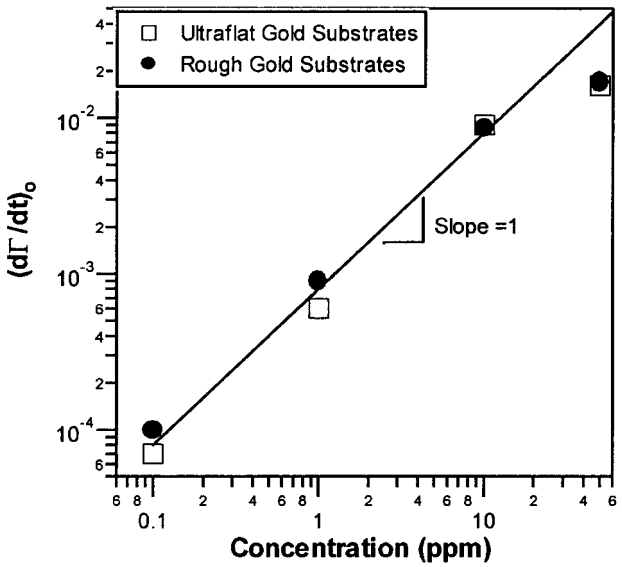

Figure 6. A log−log plot of the initial rate of adsorption of PEO as a function of bulk concentration for rough gold substrates and ultraflat gold substrates.

PEO chain has to flatten slightly on the ultraflat gold substrates to achieve contact with the surface. At small values of C_b, the mass transport rate to the surface is low, and plausibly, the chains have adequate time to flatten, which produces a slower rise in $\Gamma(t)$ (lower $(d\Gamma/dt)_0$) and smaller adsorbed amount of PEO on the ultraflat gold substrates. As the bulk concentration is increased, the supply rate to the surface becomes much larger and prevents the spreading of PEO chains. Thus, no differences are apparent in $(d\Gamma/dt)_0$ between the two cases. We aim to validate this hypothesis in the future by investigating whether a similar trend in $(d\Gamma/dt)_0$ can be observed when C_b is held constant, but the flow rate is varied to alter the supply rate of PEO to the surface.

Conclusions

In conclusion, we have performed controlled experiments on the adsorption of PEO from aqueous solutions onto planar surfaces that are physically heterogeneous but chemically homogeneous. To create surfaces that differ only in the degree of surface roughness but possess identical chemical interfaces, we have used gold substrates that are prepared by thermal evaporation on glass and by template stripping with subsequent modification by a self-assembled monolayer of a long chain alkanethiol ($CH_3(CH_2)_{11}SH$). The adsorption behavior of PEO was monitored using a surface plasmon resonance technique with high time resolution. In studies of adsorption from bulk solutions with concentration of PEO ranging from 0.1 to 50 ppm, the adsorbed amounts of PEO were found to be lower on the substrates that possessed lower roughness. The saturation coverage was consistent with a smaller distortion of the polymer chain adsorbed on the rougher surfaces. These experiments provide the first corroboration of past theoretical predictions that state that higher adsorption and lower loss of configurational entropy accompany increase in surface roughness of random surfaces. In contrast to past reports of PEO adsorption on moderately hydrophobic planar surfaces that were possibly heterogeneous, the highly hydrophobic surfaces formed by homogeneous and densely packed self-assembled monolayer of $CH_3(CH_2)_{11}SH$ induced larger adsorption of PEO. Kinetic studies revealed that the initial rate of adsorption was proportional to the bulk concentration on both rough and smooth substrates. Comparison of the adsorption on two substrates at low and high bulk concentrations suggests that the rate of spreading may affect initial rate of adsorption on the smooth substrates. PEO adsorbed more readily on the rougher surfaces, which substantiates results of past theoretical analysis.

Acknowledgment. This research was carried out with the generous support of Fredrick Seitz Materials Research Laboratory (FS-MRL) under the DOE Grant DEFG02-96ER45439 and the University of Illinois. We thank Nancy Finnegan at the FS-MRL for her help with the STM characterization.

References and Notes

(1) Fleer, G. J. *NATO ASI Ser., Ser. 3* **1996**, *18*, 269−283.
(2) Leger, L. *Macromol. Symp.* **1997**, *121*, 263−267.
(3) Fleer, G. J.; Stuart, M. A. C.; Scheutjens, J. M. H. M.; Cosgrove, T.; Vincent, B. *Polymers at Interfaces*; Chapman and Hall: London, 1993.
(4) Incorvati, C. M.; Lee, D. H.; Reed, J. S.; Condrate, R. A., Sr. *Am. Ceram. Soc. Bull.* **1997**, *76*, 65−68. Berry, A. K.; Bogan, L. E.; Agostine, S. E.; Rohm *Ceram. Trans.* **1996**, *62*, 125−132. Platonov, B. E.; Mikhailichenko, T. A.; Ryzhikov, A. P. *Kolloidn. Zh.* **1978**, *40*, 364−367. Sugiura, M. *Rept. Govt. Chem. Ind. Res. Inst., Tokyo* **1967**, *62*, 441−445. Luzinov, I.; Voronov, A.; Minko, S. *Adsorpt. Sci. Technol.* **1996**, *14*, 259−266. Gailliez-Degremont, E.; Bacquet, M.; Dauphin, J. Y.; Morcellet, M. *Colloids Surf., A* **1996**, *110*, 169−180.
(5) Ji, H.; Hone, D. *Macromolecules* **1988**, *21*, 2600−2605.
(6) Hone, D.; Ji, H.; Pincus, P. A. *Macromolecules* **1987**, *20*, 2543−2549.
(7) Gottstein, W.; Kreitmeier, S.; Wittkop, M.; Goeritz, D.; Gotsis, F. *Polymer* **1997**, *38*, 1607−1613. Xu, X.; Sun, X.; Yang, Y. *Acta Polym.* **1995**, *46*, 145−151.
(8) Douglas, J. F. *Macromolecules* **1989**, *22*, 3707−3716.
(9) Baumgaertner, A.; Muthukumar, M. *J. Chem. Phys.* **1991**, *94*, 4062−4070.
(10) Huber, G.; Vilgis, T. A. *Eur. Phys. J. B* **1998**, *3*, 217−223.
(11) Blunt, M.; Barford, W.; Ball, R. *Macromolecules* **1989**, *22*, 1458−1466.
(12) Halperin, A.; Sommer, J. U.; Daoud, M. *Europhys. Lett.* **1995**, *29*, 297−302. van der Linden, C. C.; van Lent, B.; Leermakers, F. A. M.; Fleer, G. J. *Macromolecules* **1994**, *27*, 1915−1921. Chakraborty, A. K.; Bratko, D. *J. Chem. Phys.* **1998**, *108*, 1676−1682. Heier, J.; Kramer, E. J.; Walheim, S.; Krausch, G. *Macromolecules* **1997**, *30*, 6610−6614. Balazs, A. C.; Singh, C.; Zhulina, E. *Macromolecules* **1998**, *31*, 6369−6379. Sumithra, K.; Sebastian, K. L. *J. Phys. Chem.* **1994**, *98*, 9312−9317. Andelman, D.; Joanny, J. F.; Raymond *J. Phys. II* **1993**, *3*, 121−138. Huang, K.; Balazs, A. C. *Phys. Rev. Lett.* **1991**, *66*, 620−623. Balazs, A. C.; Huang, K.; McElwain, P.; Brady, J. E. *Macromolecules* **1991**, *24*, 714−717. Odijk, T. *Macromolecules* **1990**, *23*, 1875−1876. Sumithra, K.; Baumgaertner, A. *J. Chem. Phys.* **1998**, *109*, 1540−1544. Muthukumar, M. *J. Chem. Phys.* **1995**, *103*, 4723−4731. Bratko, D.; Chakraborty, A. K.; Shakhnovich, E. I. *Chem. Phys. Lett.* **1997**, *280*, 46−52. Nath, S. K.; Nealey, P. F.; de Pablo, J. J. *J. Chem. Phys.* **1999**, *110*, 7483−7490.
(13) In past work, an experimental study on grafting of end-functionalized polymer on textured surface has been performed (see: Singh, N.; Karim, A.; Bates, F. S.; Tirrell, M.; Furusawa, K. *Macromolecules* **1994**, *27*, 2586−2594). The textured surfaces were created by spin-coating colloidal beads of various sizes on a planar substrate and then covering the beads with a layer aluminum.
(14) Ulman, A. *Chem. Rev.* **1996**, *96*, 1533−1554. Dubois, L. H.; Nuzzo, R. G. *Annu. Rev. Phys. Chem.* **1992**, *43*, 437−463.
(15) Bain, C. D.; Troughton, E. B.; Tao, Y.-T.; Evall, J.; Whitesides, G. M.; Nuzzo, R. G. *J. Am. Chem. Soc.* **1989**, *111*, 321−335.
(16) Ball, R. C.; Blunt, M.; Barford, W. *J. Phys. A: Math. Gen.* **1989**, *22*, 2587−2595.
(17) Balazs, A. C.; Huang, K. *Macromolecules* **1990**, *23*, 4641−4647.
(18) Edwards, S. F.; Muthukumar, M. *J. Chem. Phys.* **1988**, *89*, 2435−2441.

(19) Heinrich, G.; Vilgis, T. A. *Rubber Chem. Technol.* **1995**, *68*, 26−36.
(20) Rondelez, F.; Ausserre, D.; Hervet, H. *Annu. Rev. Phys. Chem.* **1987**, *38*, 317−347. Luckham, P. F. *Curr. Opin. Colloid Interface Sci.* **1996**, *1*, 39−47. Stamm, M.; Dorgan, J. R. *Colloids Surf., A* **1994**, *86*, 143−153. Penfold, J.; Richardson, R. M.; Zarbakhsh, A.; Webster, J. R. P.; Bucknall, D. G.; Rennie, A. R.; Jones, R. A. L.; Cosgrove, T.; Thomas, R. K.; Higgins, J. S.; Fletcher, P. D. I.; Dickinson, E.; Roser, S. J.; McLure, I. A.; Hillman, A. R.; Richards, R. W.; Staples, E. J.; Burgess, A. N.; Simister, E. A.; White, J. W. *J. Chem. Soc., Faraday Trans.* **1997**, *93*, 3899−3917. Cosgrove, T.; Finch, N.; Webster, J. *Colloids Surf.* **1990**, *45*, 377−389. Wang, W.; Barton, S. W. *J. Phys. Chem.* **1995**, *99*, 2845−2853.
(21) Johnson, H. E.; Granick, S. *Macromolecules* **1990**, *23*, 3367−3374. Frantz, P.; Granick, S. *Phys. Rev. Lett.* **1991**, *66*, 899−902.
(22) Malmsten, M.; Linse, P.; Cosgrove, T. *Macromolecules* **1992**, *25*, 2474−2481. Filippov, L. K.; Silebi, C. A.; El-Aasser, M. S. *Langmuir* **1995**, *11*, 872−879.
(23) Dijt, J. C.; Stuart, M. A. C.; Hofman, J. E.; Fleer, G. J. *Colloids Surf.* **1990**, *51*, 141−158.
(24) Dijt, J. C.; Cohen Stuart, M. A.; Fleer, G. J. *Adv. Colloid Interface Sci.* **1994**, *50*, 79−101. Leermakers, F. A. M.; Gast, A. P. *Macromolecules* **1991**, *24*, 718−730.
(25) Fu, Z.; Santore, M. M. *Colloids Surf., A* **1998**, *135*, 63−75.
(26) Brzoska, J. B.; Azouz, I. B.; Rondelez, F. *Langmuir* **1994**, *10*, 4367−4373.
(27) In the literature SPR has been rarely used for fundamental studies of adsorption of flexible polymers; studies of globular proteins are more common. Tassin and co-workers (see: Tassin, J. F.; Siemens, R. L.; Tang, W. T.; Hadziioannou, G.; Swalen, J. D.; Smith, B. A. *J. Phys. Chem.* **1989**, *93*, 2106−2111) have used SPR to study block copolymer adsorption on bare silver surfaces while Green and co-workers have studied pluronics on polystyrene-coated silver substrates (see: Green, R. J.; Tasker, S.; Davies, J.; Davies, M. C.; Roberts, C. J.; Tendler, S. J. B. *Langmuir* **1997**, *13*, 6510−6515).
(28) Hegner, M.; Wagner, P.; Semenza, G. *Surf. Sci.* **1993**, *291*, 39−46.
(29) Roughness of the gold substrates is measured using STM before formation of the SAMs. The monolayer formed on the gold substrate is believed to cause a renormalization of the gold surface and largely alter the surface chemistry but not the nanometer scale topography of the underlying substrate (see: Quon, R. A.; Ulman, A.; Vanderlick, T. K. *Langmuir* **2000**, *16*, 3797−3802). Several authors have reported that holes typically one gold atom deep can form during chemisorption of the alkanethiols. However, the origin of these holes remains unresolved. It is known that these holes are filled with alkanethiol molecules and do not influence the interfacial properties (see: Sondag-Huethorst, J. A. M.; Schönenberger, C.; Fokkink, L. G. J. *J. Phys. Chem.* **1994**, *98*, 6826−6834. Dishner, M. H.; Hemminger, J. C.; Feher, F. J. *Langmuir* **1997**, *13*, 2318−2322).
(30) Knoll, W. *Annu. Rev. Phys. Chem.* **1998**, *49*, 569−638.
(31) Kretschmann, E.; Raether, H. *Z. Naturforsch. A* **1968**, *23*, 2135−2136.
(32) Kooyman, R. P. H.; Lenferink, A. T. M.; Eenink, R. G.; Greve, J. *Anal. Chem.* **1991**, *63*, 83−85.
(33) Dobbs, D. A.; Bergman, R. G.; Theopold, K. H. *Chem. Eng. News* **1990**, 2.
(34) Hansen, W. N. *J. Opt. Soc. Am.* **1968**, *58*, 380−390.
(35) Past studies (see: Spanos, L.; Irene, E. A. *J. Vac. Sci. Technol. A* **1994**, *12*, 2646−2652. Spanos, L.; et al. *J. Vac. Sci. Technol. A* **1994**, *12*, 2653−2661. Liu, Q.; et al. *J. Vac. Sci. Technol. A* **1995**, *13*, 1977−1983) have shown that by using two statistical parameters such as the RMS roughness and fractal dimension a reasonably complete description of surface roughness can be provided. For surfaces that are fractal in nature ($3 > D > 2$), there is an uncertainty in the estimation of the absolute surface area because values of D larger than 2, as in our case, signify that the accessible surface area of an adsorbent changes with the size of the adsorbate (see: Erdem-Senatalar, E.; Tather, M. *Chaos, Solitons Fractals* **2000**, *11*, 953−960). In his theoretical study of an "effective surface" model for polymer adsorption, Douglas[8] has commented that instead of the absolute surface area it is the probability of intersection of the polymer chain with the "rough" fractal surface that is of importance.
(36) Almqvist, N. *Surf. Sci.* **1996**, *355*, 221−228.
(37) The fractal algorithm we use relies on dividing the surface into triangular areas of decreasing cell sizes and estimating the surface areas. The fractal dimension, D, is then estimated by a least-squares regression from a log−log plot of the surface area and the cell area.
(38) Self-assembled surfaces with advancing angles less than 46° were not used as they indicate an incomplete formation of the monolayer and thereby represent surfaces that may have chemical heterogeneity. The use of water as a probe liquid to check chemical homogeneity is also possible. $\theta_{a,water}$ is reported to be 111°−114° on a dense interface of methyl (CH_3) groups formed by self-assembled monolayers of *n*-alkanethiols (see refs 14 and 15).
(39) Past theoretical and experimental work has shown that contact angle hysteresis ($\cos \theta_a - \cos \theta_r$) increases with roughness of the substrate (see: Dettre, R. H.; Johnson, R. E. *Adv. Chem. Ser.* **1964**, *43*, 136−144. Joanny, J. F.; de Gennes, P. G. *J. Chem. Phys.* **1984**, *81*, 552−562. de Gennes, P. G. *Rev. Mod. Phys.* **1985**, *57*, 827−863).
(40) Peterlinz, A.; Georgiadis, R. *Opt. Commun.* **1996**, *130*, 260−266. DeBruijn, H. E.; Altenburg, B. S. F.; Kooyman, R. P. H.; Greve, J. *Opt. Commun.* **1991**, *82*, 425−432.
(41) Similar assumption of $n_p \sim 1.35-1.36$ has been used in past reflectivity studies of PEO adsorption on silica and is consistent with the measurements using neutron reflectivity (see: Lee, E. M.; Thomas, R. K.; Rennie, A. R. *Europhys. Lett.* **1990**, *13*, 135−141).
(42) Pagac, E. S.; Prieve, D. C.; Solomentsev, Y.; Tilton, R. D. *Langmuir* **1997**, *13*, 2993−3001.
(43) The pK_a for carboxylic-terminated SAMs has been reported to be 7.7 (see: Hu, K.; Bard, A. J. *Langmuir* **1997**, *13*, 5114−5119), and therefore, in our experiments the carboxylic terminus was not ionized.
(44) Pagac et al.[42] and Dijit et al.[23] do not report surface roughness measurements but instead report that the silicon wafers have an oxide layer of thickness 20−100 and 80−150 nm, respectively. Fu and Santore[25] have used ESCA and AFM characterization of the silica surfaces used in their investigations and have measured a surface roughness of 6 Å. It should be noted that variations in probe tip size can complicate comparison of the absolute value of roughness between different laboratories.
(45) Fadeev, A. Y.; McCarthy, T. J. *Langmuir* **1999**, *15*, 3759−3766.
(46) Devanand, S.; Sesler, J. C. *Macromolecules* **1991**, *24*, 5943.
(47) Vaneijk, M. C. P.; Stuart, M. A. C. *Langmuir* **1997**, *13*, 5447−5450. Vaneijk, M. C. P.; Stuart, M. A. C.; Rovillard, S.; Deconinck, J. *Eur. Phys. J. B* **1998**, *1*, 233−244. Stuart, M. A. C.; Fleer, G. J. *Annu. Rev. Mater. Sci.* **1996**, *26*, 463−500.
(48) Similar nonlinear concentration dependence has been reported by Fu and Santore[25] for adsorption of PEO on hydrophilic silica surfaces, where it was found that the departure from linearity occurred around 20 ppm. Fu and Santore explained that the departure was due to the fact that the high rates of adsorption at large bulk concentrations caused saturation of the surface before the local concentration gradient reached its pseudo-steady-state value.

MA001780Z